

AD-A193 176

SILICON OXIDATION STUDIES: A REVIEW OF RECENT STUDIES
ON THIN FILM SILICO. (U) NORTH CAROLINA UNIV AT CHAPEL
HILL DEPT OF CHEMISTRY E A IRENE 25 MAR 88 TR-20

1/1

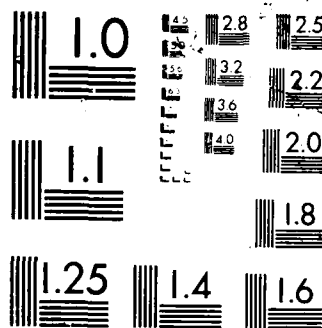
UNCLASSIFIED

N00014-86-K-0305

F/G 7/4

NL





AD-A193 176

DTIC FILE COPY (4)

OFFICE OF NAVAL RESEARCH

CONTRACT NO. N00014-86-K-0305

TECHNICAL REPORT NO. 20

Silicon Oxidation Studies: A Review of Recent Studies
on Thin Film Silicon Dioxide Formation

E. A. Irene
Department of Chemistry
University of North Carolina
Chapel Hill, NC 27514

in

The Physics and Chemistry of SiO_2 and the Si-SiO_2 Interface

DTIC
ELECTE
S APR 05 1988 D
SH

Reproduction in whole or in part is permitted for any purpose of the United States Government.

This document has been approved for public release and sale; its distribution is unlimited.

88 4 4 106

REPORT DOCUMENTATION PAGE

1a. REPORT SECURITY CLASSIFICATION Unclassified		1b. RESTRICTIVE MARKINGS													
2a. SECURITY CLASSIFICATION AUTHORITY		3. DISTRIBUTION/AVAILABILITY OF REPORT Approved for public release; distribution unlimited.													
2b. DECLASSIFICATION/DOWNGRADING SCHEDULE															
4. PERFORMING ORGANIZATION REPORT NUMBER(S) Technical Report #20		5. MONITORING ORGANIZATION REPORT NUMBER(S)													
6a. NAME OF PERFORMING ORGANIZATION UNC Chemistry Dept.	6b. OFFICE SYMBOL (If applicable)	7a. NAME OF MONITORING ORGANIZATION Office of Naval Research (Code 413)													
6c. ADDRESS (City, State and ZIP Code) 11-3 Venable Hall 045A Chapel Hill, NC 27514		7b. ADDRESS (City, State and ZIP Code) Chemistry Program 800 N. Quincy Street Arlington, Virginia 22217													
8a. NAME OF FUNDING/SPONSORING ORGANIZATION Office of Naval Research	8b. OFFICE SYMBOL (If applicable)	9. PROCUREMENT INSTRUMENT IDENTIFICATION NUMBER Contract #N00014-86-K-0305													
8c. ADDRESS (City, State and ZIP Code) Chemistry Program 800 N. Quincy Street, Arlington, VA 22217		10. SOURCE OF FUNDING NOS. <table border="1"><tr><td>PROGRAM ELEMENT NO.</td><td>PROJECT NO.</td><td>TASK NO.</td><td>WORK UNIT NO.</td></tr><tr><td></td><td></td><td></td><td></td></tr></table>		PROGRAM ELEMENT NO.	PROJECT NO.	TASK NO.	WORK UNIT NO.								
PROGRAM ELEMENT NO.	PROJECT NO.	TASK NO.	WORK UNIT NO.												
11. TITLE (Include Security Classification) SILICON OXIDATION STUDIES: A REVIEW OF RECENT STUDIES ON THIN															
12. PERSONAL AUTHOR(S) FILM SILICON DIOXIDE FORMATION		E.A. Irene													
13a. TYPE OF REPORT Interim Technical	13b. TIME COVERED FROM _____ TO _____	14. DATE OF REPORT (Yr., Mo., Day) March 25, 1988	15. PAGE COUNT 14												
16. SUPPLEMENTARY NOTATION to be published in the Physics and Chemistry of SiO ₂ and the SiO-SiO ₂ Interface															
17. COSATI CODES <table border="1"><tr><td>FIELD</td><td>GROUP</td><td>SUB. GR.</td></tr><tr><td></td><td></td><td></td></tr><tr><td></td><td></td><td></td></tr><tr><td></td><td></td><td></td></tr></table>		FIELD	GROUP	SUB. GR.										18. SUBJECT TERMS (Continue on reverse if necessary and identify by block number)	
FIELD	GROUP	SUB. GR.													
19. ABSTRACT (Continue on reverse if necessary and identify by block number) <p>The formation of thin SiO₂ films via thermal oxidation on single crystal Si substrates has been found to depend on the method of Si cleaning, impurities on the Si surface, the Si crystal orientation, film stress, and the availability of electrons at the Si surface. Recent studies on these topics are recounted along with a framework for understanding. No fully acceptable model for thin SiO₂ formation yet exists, but recent studies lead in new directions towards this goal.</p>															
20. DISTRIBUTION/AVAILABILITY OF ABSTRACT UNCLASSIFIED/UNLIMITED <input checked="" type="checkbox"/> SAME AS RPT. <input type="checkbox"/> DTIC USERS <input type="checkbox"/>		21. ABSTRACT SECURITY CLASSIFICATION Unclassified													
22a. NAME OF RESPONSIBLE INDIVIDUAL Dr. David L. Nelson		22b. TELEPHONE NUMBER (Include Area Code) (202) 696-4410	22c. OFFICE SYMBOL												

SILICON OXIDATION STUDIES: A REVIEW OF RECENT STUDIES ON THIN FILM

SILICON DIOXIDE FORMATION

Eugene A. Irene

Department of Chemistry CB 3290
University of North Carolina
Chapel Hill, N.C. 27599-3290

ABSTRACT

The formation of thin SiO_2 films via thermal oxidation on single crystal Si substrates has been found to depend on the method of Si cleaning, impurities on the Si surface, the Si crystal orientation, film stress, and the availability of electrons at the Si surface. Recent studies on these topics are recounted along with a framework for understanding. No fully acceptable model for thin SiO_2 formation yet exists, but recent studies lead in new directions towards this goal.

INTRODUCTION

From studies of the Si oxidation process in the 1960's(1-3), has come the application of the Linear-Parabolic, LP, oxidation model of Evans(4) to the SiO_2 film growth kinetics. A goodly measure of understanding was afforded to the process as a result of the application of the LP model, but even from the earliest studies(1) it was recognized that the LP model did not account for the initial oxidation regime at the outset of the oxidation of Si and extending to several tens of nm. Furthermore, even prior to oxidation and after some initial cleaning, a native oxide was observed on the Si surface. This oxide was and still is difficult to study; it forms relatively instantly, somewhat independent of ambient conditions and extends to less than 2nm in thickness. In order to account for the mysterious initial regime which included the native oxide, an offset was built into the LP model(1). This entire offset regime extends up to about 30nm in SiO_2 film thickness, L , and for ease of discussion we herein use the label L_0 for this regime, and similarly for the SiO_2 film thickness from 0nm to the native oxide thickness of less than 2 nm, we use the symbol L_0 . The L_0 regime was of little technological significance in the 1960's and early 1970's, but as device area was reduced, in order to increase device density on a chip, the SiO_2 thickness was also decreased. Now most advanced MOSFET's have gate oxides with $L < 30\text{nm}$, and recently IBM(5) showed an operating research device with $L \approx 5\text{nm}$. Thus the L_0 regime is no longer merely a scientific curiosity, and it becomes important to understand the thin film SiO_2 formation kinetics and the resultant thin film SiO_2 physical properties. This review is aimed at the present understanding of the L_0 regime.

After the usual cleaning of a Si surface (by a procedure outlined in ref 6), the Si wafer undergoes an aqueous HF dip to remove any oxide that

is formed during the cleaning process with concomitant impurities, and results in a hydrophobic surface(7) upon which a native oxide grows to about 1-2nm. Typical thermal oxidation experiments commence with the native oxide already formed, i.e. at oxidation time, t , and thickness, L : $t=0$ and $L=L_0$, and with oxidation temperatures above 800°C and usually near 1000°C, and in dry O_2 for the highest quality gate oxide or steam to accelerate oxide growth for field oxide applications. The rate of growth is observed to decrease as oxidation proceeds indicating that the growing oxide is providing a barrier to further oxidation. The SiO_2 film growth from L_0 to L_1 is characterized by faster oxidation rates than the LP regime which obtains above L_1 . Before proceeding with a detailed discussion of recent studies on the two initial regimes: 0 to L_0 and L_0 to L_1 , we briefly formulate the LP model for later use for comparison. Since this has been done many times previously(1-4,8), only the essential features are herein repeated. Firstly, we need consider the two essential processes that must occur during the thermal oxidation of Si. One process is the transport of oxidant across the growing oxide to the Si-SiO₂ interface where the oxidation reaction has been established to take place(9). This oxidant flux labeled F_1 is often approximated by a diffusive flux which at steady state is given by Fick's first law:

$$F_1 = D(C_1 - C_2)/L \quad [1]$$

where D is the oxidant diffusivity in SiO_2 , C_1 is the oxidant solubility in SiO_2 , and C_2 is the oxidant concentration at the Si-SiO₂ interface. In series with F_1 is the actual reaction between arriving oxidant and Si atoms at the Si-SiO₂ interface. This reaction is represented in its simplest form by a flux, F_2 , of formation of SiO_2 as:

$$F_2 = kC_2 \quad [2]$$

where k is a reaction rate constant and F_2 is linear in oxidant concentration. It is easy to show that a steady state will obtain for the series fluxes F_1 and F_2 , as these fluxes are self regulating. This steady state flux situation is represented in Figure 1 (10,11) in which the fluxes are plotted as linear functions of C_2 . $F_1(\max)$ is at $C_2 = 0$, and $F_2(\max)$ is at $C_2 = C_1$. The intersection of these flux lines yields the observed oxidation flux, F , which can be converted to an oxidation rate, dL/dt by:

$$dL/dt = F/\Omega \quad [3]$$

where Ω is the conversion factor for the number of O_2 's in a mole of O_2 gas to the number in a mole of solid SiO_2 which yields $\Omega = 2.3 \times 10^{22}$. The resulting integrated rate equation has linear-parabolic form as:

$$t - t_0 = (L - L_0)/k_1 + (L^2 - L_0^2)/k_2 \quad [4]$$

where t_0, L_0 represent the initial regime offset to the LP model up to L_0 of 30nm. The linear and parabolic rate constants k_1 and k_2 , respectively are defined by the following:

$$k_1 = kC_1/\Omega = k'C_1(Si)/\Omega; \quad k_2 = 2DC_1/\Omega \quad [5]$$

where the linear rate constant is written in terms of C_1 and is explicit in the Si atom concentration(12).

Using the LP model as the basis for discussion, several points are

For	
I	<input checked="" type="checkbox"/>
II	<input type="checkbox"/>
III	<input type="checkbox"/>
IV	
on/	
by Codes	
and/or	
initial	



A-1

LINEAR - PARABOLIC MODEL

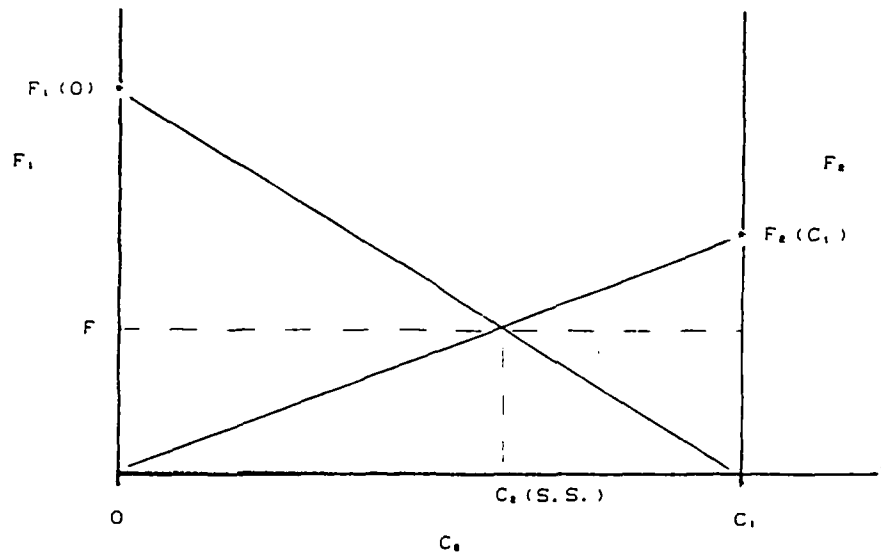


Figure 1. A representation of the diffusive flux, F_1 , and reaction flux F_2 as a function of the concentration at the Si-SiO₂ interface, C_2 . F is the steady state point (adapted from ref 11).

made which form the basis for the discussion of the Si oxidation kinetics in the initial regime of oxidation. First it must be recognized that there is no commonly accepted model for SiO₂ growth up to L_0 . Secondly, the growth regime below L_0 is comprised of two regimes: $O \rightarrow L_0$ and $L_0 \rightarrow L_0$. Thirdly, for thin SiO₂ films it is likely that the transport of oxidant is less important than the interface reaction. From Figure 1 with $F_1 \gg F_2$, the steady state point will lie on the F_2 line at a much lower value than $F_1(\text{max})$. Since the observed rate can never exceed the smaller flux, which is thought to be F_2 for the initial regime, F_2 is said to be rate limiting. Therefore, experimental studies are aimed at parameters that affect F_2 . From this, one may be tempted to argue that the dependence of the observed oxidation rate on D is nil for the initial regime, where the interface reaction is the slow step. However, Figure 1 teaches that there is a coupling between the series fluxes F_1 and F_2 as given by:

$$F = F_1 = F_2 \quad [6]$$

from which the observed rate F depends on both fluxes even if the variation of one of the fluxes is dominant. Notice from Figure 1 that a change in either F_1 or F_2 will shift the position of F irrespective of which flux is larger. With F_2 rate limiting as determined above, we now focus on specific studies of the parameters which affect F_2 , but without forgetting entirely about transport.

THE VERY INITIAL REGIME: 0 TO L_0

Since most Si oxidation experiments commence with the native oxide already present as a result of the cleaning process, and since oxidation proceeds at the Si-SiO₂ interface, thus the native oxide is replaced on the Si surface with the first formation of grown oxide, the grown oxide

is much more technologically relevant than the native oxide. However, the formation of the first oxide on the Si surface represents a regime rich in information about the mechanism of oxidation.

Several UHV studies(13-15) using optical techniques, AES and EELS have determined that the surface electronic states on the Si surface greatly decrease in number as a result of exposure to O_2 . The first step at low temperatures and exposure is the adsorption of O_2 which then converts to atomic species with increased temperature and exposure. These studies utilize Si surfaces with the oxide removed by vacuum annealing. Actual oxidation processes utilize a Si surface that has been cleaned using various but quite similar aqueous cleaning procedures(6) involving a sequence of acidic and basic H_2O_2 exposures followed by an HF exposure to remove any contaminated native oxide. It has been confirmed that these cleaning steps have a measurable effect on the oxidation kinetics(16-19). Figure 2 shows some oxidation data(18) that demonstrates that the greatest difference in oxidation rates is seen between the HF treated samples which show the largest oxidation rate and NH₄OH treated samples which show the smallest rate. Recent studies(20,21) utilized the techniques of contact angle measurement and ellipsometry, both employed in-situ in the cleaning solution media, in order to directly monitor the changes that take place during wet chemical treatments. It was found that the contact angle for a SiO_2 covered Si surface in aqueous HF changed

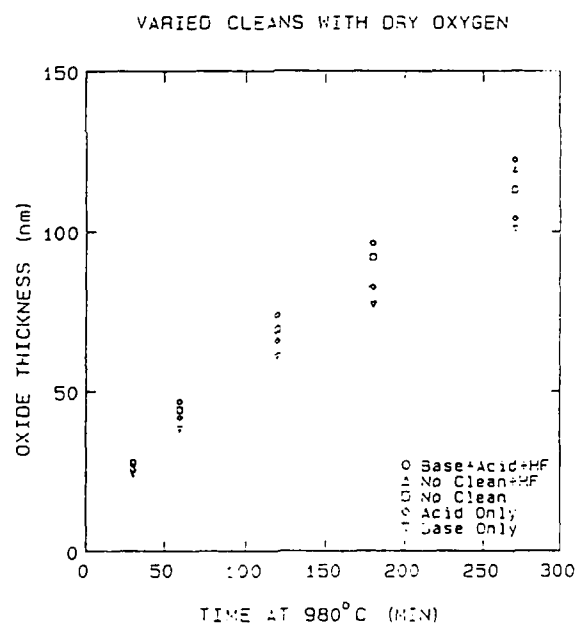
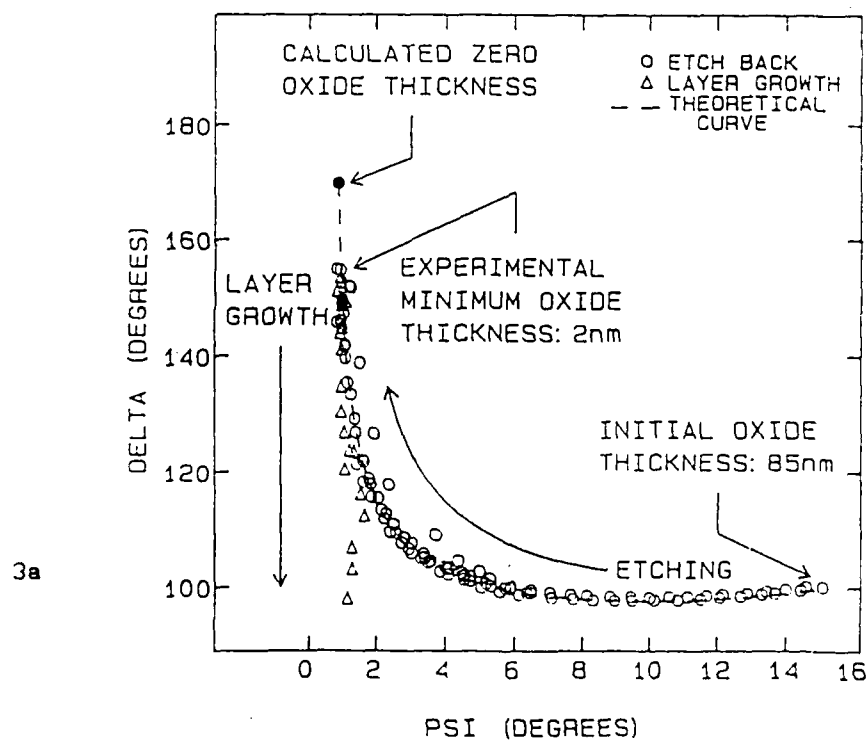


Figure 2. Comparison of Si oxidation data for various wet chemical cleaning procedures (data from ref 18)

from being hydrophilic with SiO_2 exposed to the solution, to strongly hydrophobic near the Si surface. This behavior, viz. the production of a strongly hydrophobic Si surface, has been reported(7) and is concordant with the common experience of anyone who has treated a Si surface with HF. However, based on simple thermodynamics this kind of behavior cannot be due to the bare Si surface as it has been commonly portrayed. In fact both SiO_2 and Si have high surface energies greater than 1000 dynes-cm(22), and therefore both should be strongly hydrophilic when in contact with a low energy liquid such as aqueous media with surface energies about 30 dynes-cm. The usual observation that the Si surface is hydrophobic in aqueous solutions after HF exposure is clear evidence that the HF is profoundly altering the surface of the Si. In order to investigate this alteration, the limiting contact angle technique pioneered by Zisman(23) was employed. This technique uses a homologous series of solutions with differing surface tension, and the contact angle is measured with the surface under study. The resulting data is usually found to be linear, and is extrapolated to a contact angle value of zero, which is indicative of complete wetting. The surface tension corresponding to this contact angle is called the critical surface tension and has been found to be representative of the surface structure of the solid. For HF treated Si a critical contact angle indicative of either a fluorocarbon or hydrocarbon covered Si surface was found(20). There is analytical evidence for C, H, and F on the Si surface(24-26), but at the present time we cannot unambiguously determine the chemical nature of the surface layer.

PSI vs. DELTA FOR HF ETCH EXPERIMENTS



PSI VS. DELTA FOR AMMONIA ETCH

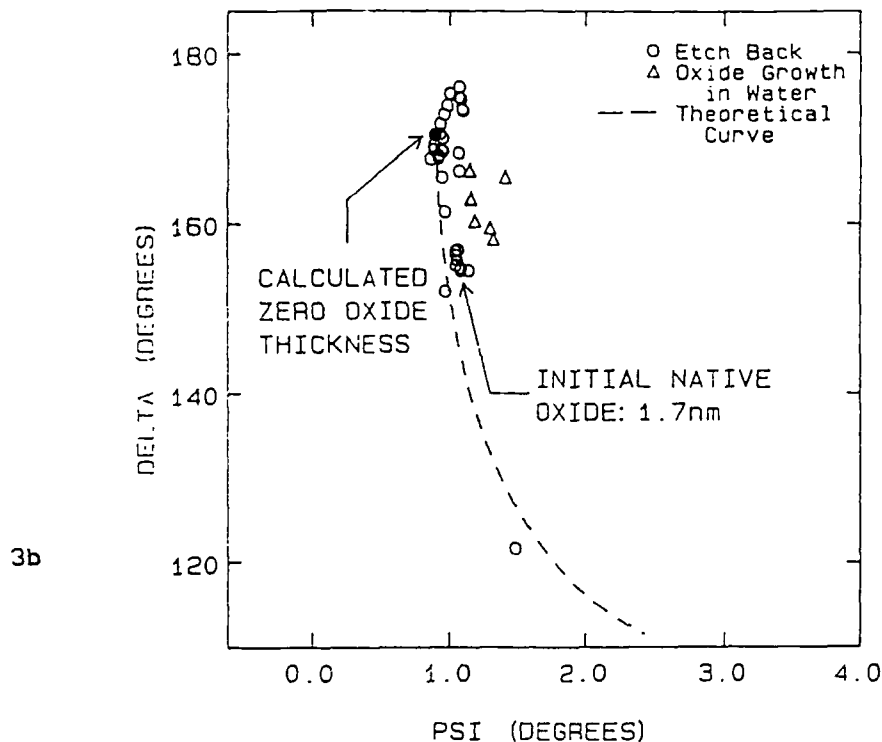


Figure 3. In-situ ellipsometric analysis of the Si-SiO₂ system exposed to a) HF-H₂O and b) NH₄OH-H₂O solutions.

In order to further elucidate the HF interaction with Si, in-situ ellipsometry was performed in HF-H₂O media on SiO₂ on Si and with some of the results shown in Fig. 3a(20). The initial SiO₂ thickness of 85nm is etched by the HF-H₂O, and the thinning is easily followed by in-situ ellipsometry with the data falling nearly identically on the theoretical Δ, ψ curve calculated for SiO₂ on Si. However, rather than the SiO₂ being etched to the bare Si surface, a minimum of about 2 nm is attained whereupon evidence is seen for layer growth, viz. Δ decreases and ψ increases (slightly). Presumably the HF removes the SiO₂, but it is replaced with a new film which renders the Si surface strongly hydrophobic. This result is contrasted with the effects of NH₄OH-H₂O on SiO₂ on Si as shown in Fig. 3b(21). In this case, the SiO₂ etching, much slower than in HF-H₂O, results in an apparently bare Si substrate with no film formation. It is believed that the scatter in the Δ, ψ data about the bare Si surface point is due to the observed roughening of the Si surface when exposed to NH₄OH. It then appears that the hydrophobic Si surface, for reasons not yet established, enhances the Si oxidation rate over the bare surface.

The very initial oxidation regime is fast, i.e., the native oxide forms virtually instantly at room temperature and to a thickness of about 1 nm. After this formation, further growth to 2 nm is relatively slow. It appears that the native oxide film formation may be due to surface electronic effects and related to the charge available in surface electronic states, but a discussion of this is delayed until electronic effects are discussed in the next section. Recently, a number of studies(16-21) have revived earlier work(27-29) that showed that

impurities have a profound effect on the initial oxidation kinetics. Indeed most impurities increase the propensity and speed of oxidation. The older work showed that Na, the ubiquitous impurity that plagued the early development of the technology, increased the oxidation rate. Even trace amounts by chemical analysis standards had measurable effects. No real mechanism was deduced but effects on the interface reaction and the diffusion of oxidant were deemed likely from the analysis of the oxidation data in terms of the LP model. Systematic studies with H_2O additions to an O_2 oxidation ambient(30) have demonstrated that trace amount effects on the oxidation rate were proportionately larger than for substantial H_2O additions to O_2 , and that both the interface reaction and the transport of oxidant through the film were enhanced by the presence of H_2O as obtained from applications of the LP model. More recent UHV studies with sub monolayers of Ag and Au on Si(31) report that the electronic nature of the impurity and surface interaction is important. In particular both Ag and Au were found to be deposited on (111) Si in a disordered state, and appeared to form a metal like surface on Si, as evidenced by a high density of electron states at the Fermi level. This kind of surface was found to oxidize readily when exposed to O_2 . On the other hand, when heated, these metal-like disordered surfaces became ordered and semiconductor-like with a low density of states at the Fermi level, and under these conditions hardly oxidized at all. Similar oxidation enhancement effects were found for Cs and Na(32) and were attributed to metallization of the surface and a tendency towards producing atomic oxygen. Other work with K(33) also shows an oxidation enhancement, but the effect was thought to be due to an efficient transfer of O atoms to the Si surface, since the formation of K oxides was found and the SiO_2 formation was found to occur below the K layer. Si oxidation enhancement effects were also recently reported for Cu(34), Pd(35), Cr(36) and Cs(37), and other older reports are in the literature. We return to these ideas later after other enhancement effects are introduced.

THE INITIAL REGIME: L_0 TO L_1 .

This regime extends to about 30 nm in SiO_2 film thickness, and due to device scaling considerations has recently become the focus of technological importance for gate oxide applications in MOS technology (38). Also, this regime is characterized by fast oxidation rates, relative to the L-P regime which follows, but not so fast as to be difficult to measure, as is the case for the very initial regime, $O \rightarrow L_0$. Hence, there exists a goodly number of careful oxidation kinetics investigations yielding copious film growth data for study(8, 39-42).

From the data, it is clear that this regime, which is sometimes referred to as the "linear" regime never displays purely linear film growth kinetics. The oxidation rate decreases in time similar to the L-P regime, but more slowly. There have been numerous attempts to fit the data to one kind of oxidation model or another. Rather than review these attempts which are technologically important for process models, but which are not usually scientifically rewarding, some of the important physical processes are identified through the use of a variety of experimental techniques.

Figure 4a shows oxidation data for the three low index Si orientations and for the entire L_0 regime. The non linearity is clear as is a pronounced orientation dependence(12, 40-42) over the temperature range studied of 600 to 1100°C. From a comparison of Figs. 4a and 4b

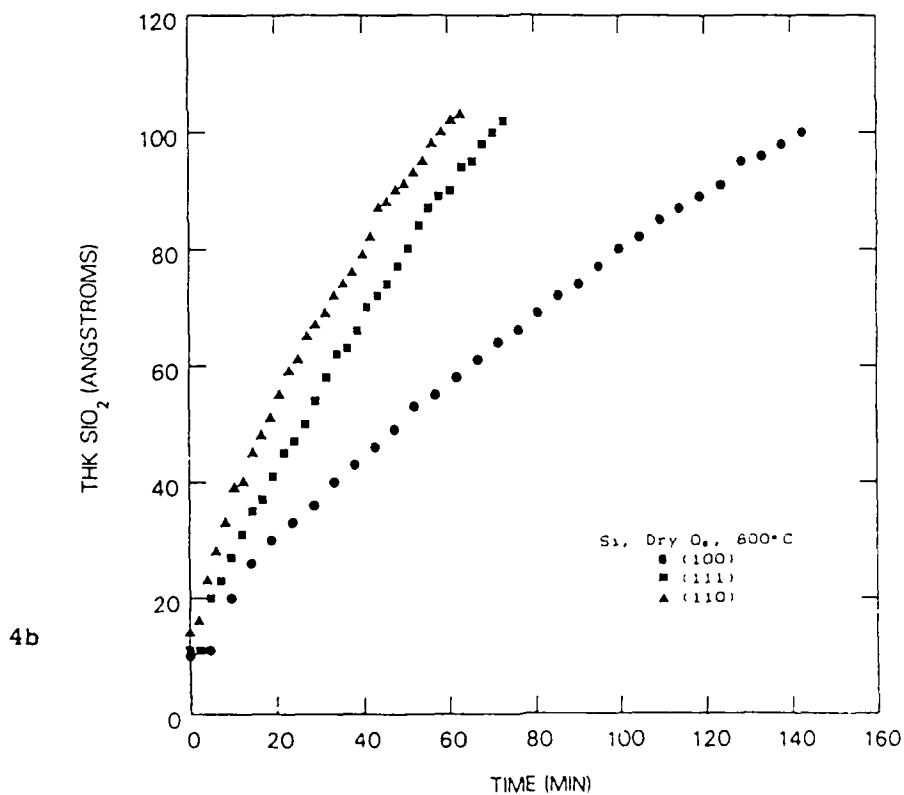
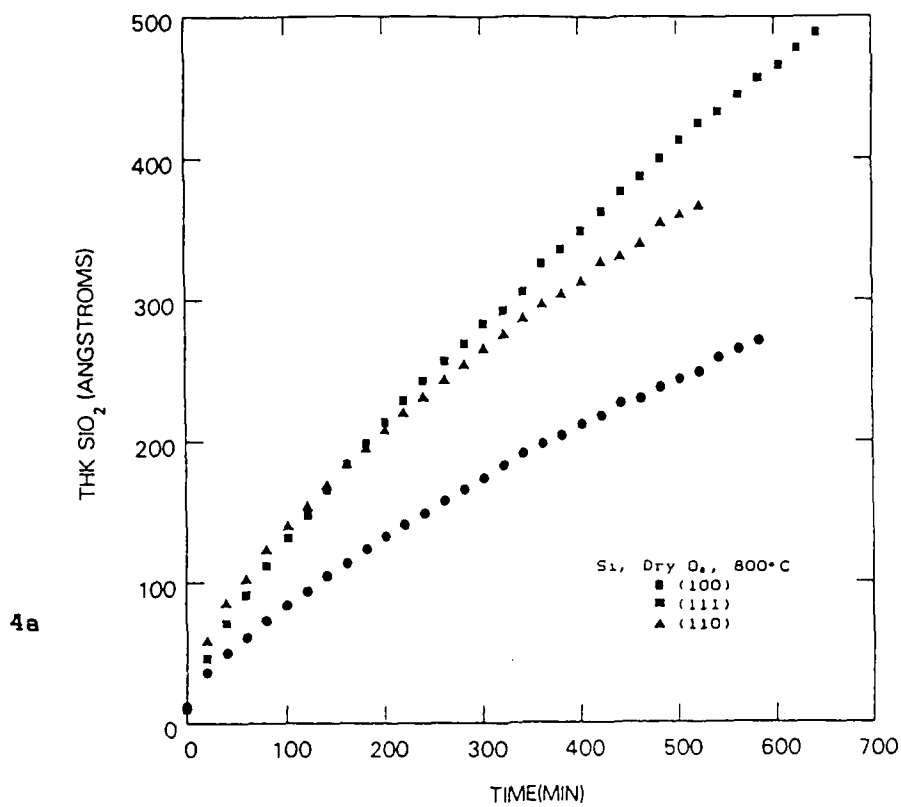


Figure 4. Comparison of Si oxidation data for the (111), (110) and (100) Si orientation for dry O_2 at 800°C for a) the range of 0 to 500 Å SiO_2 thickness and b) the same data with the 0 to 100 Å region expanded (from ref 12 and with permission of the Electrochemical Soc. Inc.).

which is the same data but with only the first 10 nm plotted in 4b, we observe the following orientation behavior for the oxidation rates, R:

0 to 15 nm: $R(110) > R(111) > R(100)$

15 nm upwards: $R(111) > R(110) > R(100)$

From this data, two questions arise: why the initial order and why the crossover between the (111) and (110) orientations as the oxide grows? The first question is answered by reference to equation [5] for k_1 , which is a function of the Si surface concentration. It has been established(41-43) that the order for the Si atom areal density is as follows:

$(110) > (111) > (100)$

Thus the initial rates scale at least qualitatively according to eqn. [5] with $[Si]$. More complete recent work(41,42) on the Si orientation effect which included the (311) and (511) as well as the three major orientations also show that the initial oxidation rates up to at least 10nm scale with the Si surface atom density, $[Si]$. The second question is answered with less confidence. If it is considered that there is a compressive stress in the SiO_2 , which can reduce D, then the orientation which exhibits the lowest SiO_2 compressive stress might be expected to exhibit the largest oxidation rate when the SiO_2 is sufficiently thick for the stress to be efficacious(42).

Figure 5 shows the SiO_2 intrinsic film stress as a function of oxidation temperature and for four orientations(44). Germane to the orientation dependence of the oxidation rate discussed above, it is seen that the (111) Si exhibits the lowest stress at all oxidation temperatures and should be expected to yield the largest oxidation rate, as is observed. However, while this interesting correlation provides a starting hypothesis, it remains to be conclusively established whether intrinsic stress really effects oxidation. One recent study suggests such a relation(45) by comparing the oxidation rate for 100nm SiO_2 covered samples, half of which have an intrinsic and half have had the stress relieved, with the finding of a higher rate for the stress relieved samples.

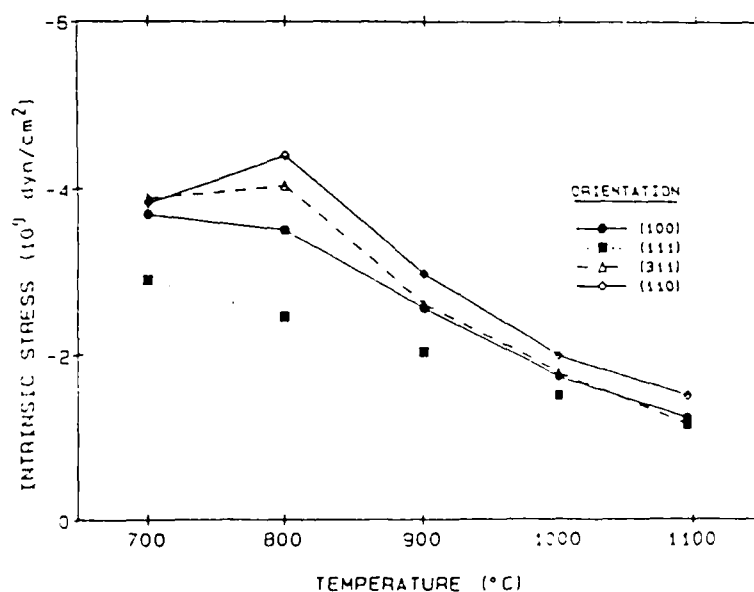


Figure 5. Measured intrinsic SiO_2 film stress as a function of oxidation temperature for four Si orientations (from ref 44 and with permission of the Am. Inst. Physics).

Two additional factors relative to stress effects on oxidation are worthy of further attention. One is the temperature dependence of the stress as is seen in Figure 5, and the other is the possible effect on the interface reaction. The considerable increase in intrinsic stress for lower oxidation temperatures suggests that the oxide viscosity which also increases sharply with decreasing temperature may be implicated. A viscous flow model for oxidation was proposed(46) based on earlier similar research(47). Figure 6 shows that according to the viscous flow model the SiO_2 formed flows normal to the Si surface in response to the lateral compression with a rate of flow proportional to the ratio of stress to viscosity. This relationship arises from considering the SiO_2 to be a Maxwell solid. Also, an oxidation model was proposed(12,48) for the initial regime where the rate of oxidation may scale with the rate at which the SiO_2 can relax. Very recent stress measurements(49) which compared as-grown SiO_2 film from 10 to 100 nm with similar thicknesses of SiO_2 but etched back from a starting 100 nm SiO_2 film revealed the same stress distribution, stress levels, and the same limiting value for stress at zero oxide thickness. The stress distribution shows a modest increase of less than a factor of two in intrinsic stress near the SiO_2 -Si interface. The fact that the same values for the intrinsic stress are obtained from the two experiments means that once the oxide is formed, there is only very slow SiO_2 relaxation even with the vastly different oxidation rates for the formation of the thin SiO_2 films in the two experiments. The limiting stress value of between $4\text{-}5 \times 10^9$ dynes/cm² is more than an order of magnitude less than the maximum stress(46), and strongly suggests that there exists a low viscosity for the initially grown SiO_2 , but this low value relaxes to a much higher viscosity value when the SiO_2 network is well formed. In this way a rapid initial relaxation lowers the stress, but then is followed by a slower relaxation rate in conformity with the equilibrium SiO_2 viscosity.

The possible effect of this stress on the interface reaction has been modeled(12,46,48) under the assumption that SiO_2 is a Maxwell solid. The essential idea is that the large molar volume change which attends the conversion of Si to SiO_2 , and is responsible for the intrinsic stress, also couples into the interface reaction rate constant. To accomplish this, equation (5) is rewritten as follows:

$$k_i = k' C_i [\text{Si}] / \Omega = k' C_i [\text{Si}^*] / \Omega \quad (6)$$

where $[\text{Si}^*]$ is the effective Si concentration and given by $[\text{Si}]$, the areal density of Si atoms reduced by multiplying by the rate at which the SiO_2 flows away from the Si surface during oxidation. For a Maxwell solid this fraction is the strain rate, $\dot{\epsilon}$, which is given as:

$$\dot{\epsilon} = \sigma / \eta \quad (7)$$

where σ is the intrinsic stress as usual, and η is the oxide viscosity. Then k_i becomes:

$$k_i = k' C_i [\text{Si}] \sigma / \eta \quad (8)$$

and the initial regime dominant rate process is a function of the rate of relaxation of the as-forming SiO_2 .

There appears to be a growing body of experimental evidence that indicates that the electronic nature of the Si surface determines the initial Si oxidation rates. The evidence to be discussed herein is based on photonic effects, metallic Si surfaces and impurities.

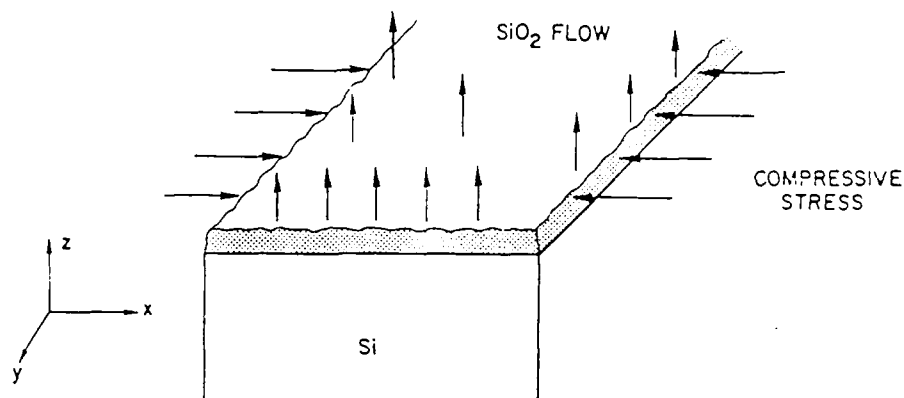


Figure 6. Viscous flow model for Si oxidation (from ref 46 and with permission of the Electrochemical Soc. Inc.

A number of studies(50-55) attest to the Si oxidation enhancement effects of intense light, usually laser light, on the oxidation of Si. Very recent results(53) estimate a 20-25% enhancement of the oxidation rate for 800°C oxidation using the 514.5 and 488 nm lines from an Ar ion laser. A number of models have been proposed, in order to explain the results. In one model the flux of excited electrons in Si over the Si-SiO₂ barrier is compared with the enhanced oxidation rate(54) and reasonable agreement is found. The photonically excited electrons are thought to assist in the decomposition of molecular oxygen and thereby accelerate the reaction. A similar mechanism but without photon enhancement of electrons was considered as a possibility to occur for the thermal oxidation of Si(56). In order to carefully test this model for thermal oxidation, oxidation data in the very initial oxidation regime of up to 5 nm was obtained and compared with the calculated thermionic flux of electrons(56). The agreement was found to be quite good for oxide growth less than 5 nm and for oxidation temperatures from 600 to 1100°C. Essentially, the thermionic oxidation model for the very initial thermal oxidation regime is as follows:

1. In the Si conduction band: $\text{Si} \rightarrow \text{Si}^* + e^-$
2. At the Si-SiO₂ barrier: $e^-(\text{Si C.B.}) \rightarrow e^-(\text{SiO}_2 \text{ C.B.})$
3. In SiO₂: $\text{O}_2(\text{at the Si-SiO}_2 \text{ interface}) + e^- \rightarrow \text{O}^- + \text{O}$
4. The Interfacial Reaction: $\text{Si}^* + \text{O}^- + \text{O} \rightarrow \text{SiO}_2$

with step 2. being rate limiting. We will return to this model to attempt correlation with the other oxidation effects which seem to effect the barrier, and thus affect the oxidation rate. For thicker films the transport of oxidant and other parameters discussed above cannot be ignored, as was discussed above. Also in this study(56) the role of electrons in intrinsic Si surface electronic states was found to be about the correct number to explain the initial very rapid formation of 1nm of native SiO₂ on Si, the L₁ layer with the assumption that one electron in a surface state could be available for the oxidation reaction without the need for thermionic emission over the Si-SiO₂ barrier. Other models have used the idea of surfaces states or dangling bonds but these models have usually been used to explain the formation of oxide thicker than L₁(55, 57).

The previously mentioned reports(31-37) show that metallic impurities of less than a monolayer accelerate the Si oxidation rate, strongly support the notion that the metallicity of the Si surface is crucial for the observed oxidation enhancements. In further support of this idea are recent reports(58,59) that a wide variety of metal silicides exhibit decidedly different oxidation behavior according to the electronic nature of the silicide surface. The oxidation of the variety of metal silicides was performed such that there was an ample supply of Si from the Si substrate underneath the silicide, and under oxidations conditions that yielded only SiO_2 on the silicide surface and the thickness of the silicide was preserved. In effect it is Si oxidation but on a silicide surface. Figure 7 summarizes these experimental results in which three bands of oxidation behavior is identified which correlate with the optical absorption of the silicide surfaces. The fastest oxidizing silicides exhibit the largest optical absorption as measured by ellipsometry, and the slowest oxidizing silicides oxidize at about the same rate as Si and these silicides are thought to be semiconducting silicides(58). The optical absorption in the visible is another measure of the surface metallicity with the greatest absorption attributed to a greater free electron concentration. These silicide oxidation experiments enable the oxidation of Si to occur on surfaces with decidedly different electronic properties.

Impurities on the Si surface usually increase the initial Si oxidation rate. Without impurities the initial rate is accounted for by the thermionic emission of electrons over the Si-SiO₂ interface. For consistency with this model, it is argued that the impurities alter the barrier, usually resulting in a lower barrier as would be expected for impurities on any surface and some precedent for this exists(60).

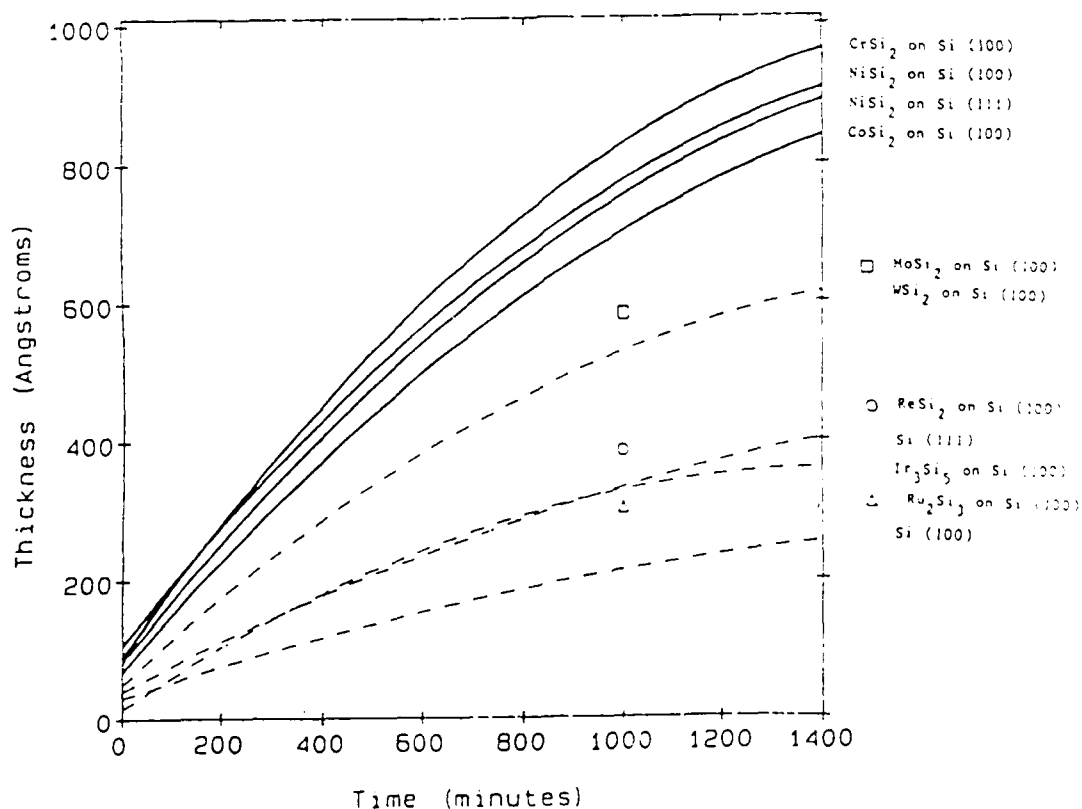


Figure 7. Oxidation behavior of a variety of metal silicides on Si oxidized at 750°C in dry O₂ and compared with pure Si (data from ref 59).

CONCLUSIONS

The initial Si oxidation regime remains without an accepted physical model. New experimental studies implicate impurities, cleaning procedures, the electronic nature of the Si surface, the crystallography of the surface, and mechanical stress as possible phenomena bearing on the physical processes that take place for the initial thin SiO₂ oxidation regime. Both the number and barrier for surface electrons appear to be important. These recent studies provide new paths for future Si oxidation research.

ACKNOWLEDGEMENTS

This work was supported in part by the Office of Naval Research, ONR, and the IBM corporation.

REFERENCES

1. B.E. Deal and A.S. Grove, J. Appl. Phys., **36**, 3770 (1965).
2. W.A. Pliskin, IBM J. Res. and Develop., **10**, 198 (1965).
3. A.G. Revesz, K.H. Zaininger and R.J. Evans, J. Electrochem. Soc., **113**, 706 (1966).
4. U.R. Evans, "The Corrosion and Oxidation of Metals", Arnold, London (1960).
5. R. Rosenberg, Abstract DG-TUM2, presented at 34th AVS meeting Anaheim, CA, Nov. 2-6, 1987.
6. W. Kern and D.A. Poutinen, RCA Rev., **31**, 187 (1970).
7. R. Williams and A.M. Goodman, Appl. Phys. Lett., **25**, 531 (1974).
8. E.A. Irene and Y.J. van der Meulen, J. Electrochem. Soc., **123**, 1380 (1976).
9. J.R. Ligenza and W.G. Spitzer, J. Phys. Chem. Solids, **44**, 131 (1960).
10. V.G. Levich, "Physicochemical Hydrodynamics", Prentice Hall, Englewood Cliffs, N.J. (1962), pp. 72-78.
11. E.A. Irene and R. Ghez, Appl. Surface Sci., **30**, 1 (1987).
12. E.A. Irene, H.Z. Massoud and E. Tierney, J. Electrochem. Soc., **133**, 1253 (1986).
13. P. Chiaradia and S. Nannarone, Surface Science, **54**, 547 (1976).
14. J. Derrien and M. Commandre, Surface Science, **118**, 32 (1982).
15. H. Ibach, H.D. Bruckmann, and H. Wagner, Appl. Phys. A, **29**, 113 (1982).
16. F.N. Schwettman, K.L. Chiang and W.A. Brown, 153rd Electrochemical Society Meeting, Abstract 276, May 1978.
17. F.J. Grunthaner and J. Maserjian, IEEE Trans. Nucl. Sci., **NS-24**, 2108 (1977).
18. G. Gould and E.A. Irene, J. Electrochem. Soc., **134**, 1031 (1987).
19. J.M. DeLarios, C.R. Helms, D.B. Kao and B.E. Deal, Appl. Surface Sci., **30**, 17 (1987).
20. G. Gould and E.A. Irene, J. Electrochem. Soc., accepted for publication (1988).
21. G. Gould and E.A. Irene, J. Electrochem. Soc., submitted 1988.
22. W.A. Zisman, "Contact Angle: Wettability and Adhesion", in Advances in Chemistry Series, Vol. 43, Ed. F.M. Fowkes, Am. Chem. Soc., Washington, D.C. (1964), Chap. 1.
23. H.W. Fox and W.A. Zisman, J. Colloid Sci., **5**, 514 (1950).
24. G.B. Larrabee, K.G. Heinen and S.A. Harrell, J. of Electrochem. Soc., **114**, 867 (1967).
25. E. Yablonovitch, D.L. Allara, C.C. Chang, T. Gmitter and T.B. Bright, Phys. Rev. Lett., **57**, 249 (1986).
26. R.E. Benenson, L.C. Feldman and B.G. Bagley, Nuclear Inst. and Methods, **168**, 547 (1980).

27. A.G. Revesz and R.J. Evans, J. Phys. Chem. Solids, 30, 551 (1969).
28. E.A. Irene, J. Electrochem. Soc., 121, 1613 (1974).
29. Y.J. van der Meulen and J.G. Cahill, J. Electronic Materials, 3, 371 (1974).
30. E.A. Irene and R. Ghez, J. Electrochem. Soc., 124, 1757 (1977).
31. A. Cros, J. Physique, 44, 707 (1983).
32. A. Franciosi, P. Soukiassian, P. Philip, S. Chang, A. Wall, A. Raisanen and N. Troullier, Phys. Rev. B, 35, 910 (1987).
33. M.C. Asensio, E.G. Michel, E.M. Oellig, and R. Miranda, Appl. Phys. Lett., 51, 1714 (1987).
34. P.J. Moller and J. He, J. Vac. Sci. Technol. A, 5, 996 (1987).
35. G. Abbati, L. Rossi, L. Calliari, L. Braicovich, I. Lindau and W.E. Spicer, J. Vac. Sci. Technol., 21, 409 (1982).
36. P. Wetzel, C. Pirri, J.C. Peruchetti, D. Bolmont and G. Gewinner, J. Vac. Sci. Technol. A, 5, 3359 (1987).
37. P. Soukiassian, T.M. Gentle, M.H. Balshi and Z. Huryck, J. Appl. Phys., 60, 4339 (1986).
38. E.A. Irene, "Semiconductor International", p. 99, April 1983 and p. 92, June 1985.
39. M.A. Hopper, R.A. Clarke, and L. Young, J. Electrochem. Soc., 122, 1216 (1975).
40. H.Z. Massoud, J.D. Plummer and E.A. Irene, J. Electrochem. Soc., 132, 1745, 2685 (1985).
41. E.A. Lewis, E. Kobeda and E.A. Irene, in "Semiconductor Silicon 1986." H.R. Huff, T. Abe and B. Kolbeson, Eds. p. 416, The Electrochemical Soc., Pennington, N.J. (1986).
42. E.A. Lewis and E.A. Irene, J. Electrochem. Soc., 134, 2332 (1987).
43. J.R. Ligenza, J. Phys. Chem., 65, 2111 (1961).
44. E. Kobeda and E.A. Irene, J. Vac. Sci. Technol., 85, 15 (1987).
45. J.K. Srivastava and E.A. Irene, J. Electrochem. Soc., 132, 2815 (1985).
46. E.A. Irene, E. Tierney and J. Angillelo, J. Electrochem. Soc., 129, 2594 (1982).
47. E.P. EerNisse, Appl. Phys. Lett., 30, 290 (1977); 35, 8 (1979).
48. E.A. Irene, J. Appl. Phys., 54, 5416 (1983).
49. E. Kobeda and E.A. Irene, J. Vac. Sci. Technol. B, accepted for publication 1987.
50. R. Oren and S.K. Ghandi, J. Appl. Phys., 42, 752 (1971).
51. S.A. Schafer and S.A. Lyon, J. Vac. Sci. Technol., 13, 494 (1981); 21, 422 (1982).
52. Ian W. Boyd, Appl. Phys. Lett., 42, 728 (1983).
53. F. Micheli and Ian W. Boyd, Appl. Phys. Lett., 51, 1149 (1987).
54. E.M. Young and W.A. Tiller, Appl. Phys. Lett., 42, 63 (1983); 50, 46 (1987); 50, 80 (1987).
55. P. Quenon, M. Wautelet, and M. Dumont, J. Appl. Phys., 61, 3112 (1987).
56. E.A. Irene and E.A. Lewis, Appl. Phys. Lett., 51, 767 (1987).
57. S.A. Shafer and S.A. Lyon, Appl. Phys. Lett., 47, 154 (1985).
58. F.M. d'Heurle, A. Cros, R.D. Frampton and E.A. Irene, Philos. Mag. B., 55, 291 (1987).
59. R.D. Frampton, E.A. Irene and F.M. d'Heurle, J. Appl. Phys., 62, 2972 (1987).
60. M. Liehr, P.E. Schmid, F. K. Le Goues, and P.S. Ho, J. Vac. Sci. Technol., A4, 855 (1986).

END
DATE
FILMED
DTIC
JULY 88